Residence Time Distributions in a Stirred Tank: Comparison of CFD Predictions with Experiment

Byung S. Choi,[†] Bin Wan,[†] Susan Philyaw,[†] Kumar Dhanasekharan,[‡] and Terry A. Ring*[,†]

Department of Chemical Engineering, University of Utah, 50 South Central Campus Drive, Salt Lake City, Utah 84112, and Fluent, Inc., 10 Cavendish Court, Centerra Resource Park, Lebanon, New Hampshire 03766-1442

Residence time distributions (RTD) are measured for both a baffled and an unbaffled laboratory reactor of the same size with several internal pipes and a Rushton turbine operating at different feed flow rates and impeller rpms. Ideal behavior as determined by the mean and the variance of the RTD was observed at an impeller Reynolds number of 2327 for the baffled tank and 3878 for the unbaffled tank both in the turbulent transition range. The experimental results for the baffled tank are compared to computational fluid dynamics (CFD) predictions of the RTD using the $k-\epsilon$ turbulence model in Fluent for transitional flow regime in the tank, i.e., impeller Reynolds number between 10 and 10 000. All the qualitative aspects of the predicted RTDs are similar to those measured experimentally. The mean residence times as well as the variances of the residence time are accurately predicted by CFD in the transition flow regime.

Introduction

Continuous stirred tanks are used ubiquitously in the chemical process industry for mixing, reactions, and crystallizations. The mixing in a continuous stirred tank is often not ideal. The residence time distribution (RTD) is one of the ways to characterize the nonideal mixing in the tank. Comparison of the measured RTD with that of an ideal reactor allows the process engineer to diagnose the ills of the tank and mixer design. The engineer can then use an appropriate mixing model for the tank in combination with the kinetics of the reaction to be performed in the tank to develop an appropriate model for the reactor.[1]

Constant stirred tank mixers and reactors have been the focus of various RTD studies over the years. Experiments carried out by Khang and Levinspiel,[2] Zaloudik,[3] and Gianetto and Cazzulo[4] for constant stirred tanks of standard size (diameter equals height) with standard baffle[5] designs and various impeller designs have been done for a broad range of tank sizes, feed flow rates, and impeller rpms. These studies show a transition from nonideal to ideal RTD behavior as rpm is increased. Idealized RTDs are always observed for an impeller Reynolds number in the transition flow regime, with the critical Reynolds number depending upon the type of impeller being used and the baffle structure. Various theories have been presented to predict the RTD for nonideal RTDs including one and two parameter models[1] and three and higher parameter models.[4,6−8] These higher parameter models consider by-pass, dead zones, recycle, ideal back mixed regions, and plug flow regions. These models have been used to predict the nonideal RTD,[2−9] the performance of reactors operating with various chemical reactions,[10−12] and nonideal reactor scale-up.[4,13]

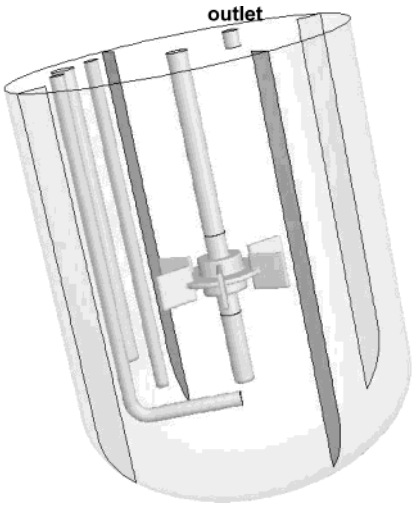

Figure 1. Reactor geometry.

This work measures the RTD of a laboratory reactor both with and without baffles and makes comparisons of these measurements with predictions for the RTD using computational fluid dynamics (CFD) with a $k-\epsilon$ turbulence model coupled with a dynamic two-species, fluid and tracer, mass balance operating with a step change of the concentration of tracer in the feed.

Experimental Section

The geometry of the ∼1.4 L laboratory baffled stirred tank reactor is shown in Figure 1 with all internal dimensions given in Table 1. For the unbaffled experiments the baffles were removed and the tank was filled to ∼1.3 L. The baffled tank has four baffles of conventional thickness, a Rushton turbine, and three internal pipes protruding into the reactor from its top, two of which are feed ports and one of which is a thermal well. One of the feed tubes dead-ends at the approximate height of the impeller and was not used in these

* To whom correspondence should be addressed. Tel.: (801) 585-5705. Fax: (801) 585-9291. E-mail: ring@eng.utah.edu.
[†] University of Utah.
[‡] Fluent, Inc.

10.1021/ie0308240 CCC: $27.50
Published on Web 08/27/2004

Table 1. Dimensions of Tank, Baffles, Rushton Impeller, and Internal Tubes

	description	dimension (mm)
vessel	vessel diameter, D	114
	vessel height, H	145
baffle	baffle width, W	9.5 (= D/12)
	baffle thickness, T	2.5
	gap between wall and baffle, G_w	1.6 (∼D/72)
	gap between vessel and baffle, G_v	2.4 (∼W/4)
impeller	blade height	11.25
	blade width	11.25
	blade thickness	1.5
	diameter	45
internal tubes	centered between two baffles angle covered by all 3 internal tubes	45°
inlet tubes (2)	inside diameter	1.6
	outside diameter	3.5
	radial position of centerline	40
central internal tube (thermal well)	outside diameter	5
	radial position of centerline	40
outlet tube (tank top)	inside diameter	1.6
	outside diameter	4.5
	radial position of centerline	46

experiments; the other tube is bent to feed directly below the impeller. Also protruding ever so slightly into the top of the liquid are the outlet tube, a pH probe, conductivity probe, thermocouple, potassium-specific ion electrode, and level indicator (not shown in Figure 1). The reactor output flows directly into a flow cell of a UV−Vis spectrometer operated at a fixed wavelength. All of these instruments, as well as the feed pump, product pump, the jacket feed temperature, thermal well temperature, and the rpm and torque on the stirrer, were connected to an OPTO-22 data acquisition and control system collecting data at time intervals of 1 s. The reactor control system has the capability of controlling the feed source and reactor temperature to ±0.25 °C, the feed and product flow rate to ±0.5 mL/min, the liquid level to ±3.9 mm, and the mixing speed to ±3 rpm.

The ratio of liquid level to the tank diameter (H/D) of the vessel in Figure 1 is 1.27 is within the general range of 1.0 to 1.5 for most industrial stirred tank precipitators.[14,15] To reduce the energy input to the system while maintaining mixing uniformity, a standard baffle design[5] was used consisting of four flat vertical plates, radially directed (i.e., normal to the vessel wall), spaced at 90° around the vessel periphery running the length of the vessel's straight side. Standard baffle widths are between $^1/_{10}$ and $^1/_{12}$ of the vessel diameter (D/10 or D/12), see Table 1 for details. The gaps with the vessel wall and base are left to allow the flow to clear the baffles. Recommended gaps are equal to $^1/_{72}$ of the vessel diameter (D/72) between the baffles and the vessel wall, and $^1/_4$ to one full baffle width between the bottom of the baffles and the vessel base. More of the detailed baffling information could be found in Kevin, et al.[16] Stirring was achieved by a six-bladed Rushton turbine. The dimensions of the turbine are also given in Table 1.

The rpm of the peristaltic pumps is controlled by an Opto 22 control system establishing the feeding and removal of product solution from the tank. Flow rate was obtained by the careful and repeated calibration of the speed of pump and tube size to ensure the desired feed and withdrawal rates as well as a constant residence time. The Opto 22 computer also measured the on-line sensor quantities: temperature, pH, absorbance, and conductivity, as well as potassium ion concentration. All of these measurements were used to monitor the concentration of the tracer inside and exiting the reactor. The calibration for all of these systems was done before each run to ensure measurement accuracy. The RTD measured was the combination of process dynamics and sensor dynamics.[17] The sensor dynamics are much faster than that of the process. The sensor time constants are the following: conductivity, which has a measurement time of 1 s; K^+ ion and pH, which have measurement times of 4−8 s; absorbance, which has a measurement time related to the flow rate through the absorbance sample cell, or at worst 10 s; and temperature, which has a measurement time of 0.5 s.

Measurement of the RTD. The RTD is determined experimentally by injecting a 10 mL volume of inert multicomponent chemical tracer (a hot solution of 0.1 gm/L methyl blue dye, 50 gm/L NaCl, 20 gm/L KCl, and 3.6 gm/L HCl with water) into the tank at time zero. In all experiments, the feed tube was the bent one that fed just below the impeller. On-line analyzers detected each of the species in the tracer; blue dye with the aid of a video camera[18] and UV-vis spectrometer, temperature with a thermocouple, salt with conductivity, and H^+ concentration with pH meter were measured simultaneously with various conditions such as different flow rates and mixer rpm values. Great care was used in synchronizing the pulse input with the initiation of data accumulation for RTD analysis and to calibrate the pumps to ensure that the reactor space−time [= V_{tank}/Q] was accurately measured. A listing of all the experimental conditions used to measure RTDs is given in Table 2 (part a for the without-baffle experiments and part b for the with-baffles experiments). Table 2a also gives the impeller Reynolds number, and Table 2b gives the impeller Reynolds number and impeller power number, calculated from the measurement of the impeller torque. For all of these experiments data were taken at 1-s intervals. Figures 2 and 3 illustrate bad mixing at 0 rpm and good mixing at 287 rpm for the tank without baffles as measured by conductivity, pH and temperature. The UV-vis spectrometer data and K^+ ion data are not shown in these figures, however, they are similar to those for the other curves presented in these figures. All of these curves show a fast increase at an early time followed by an exponential decrease as expected for a continuous stirred tank. The delay of the

Table 2. Experimental Conditions for RTD Measurements Without Baffles and With Baffles

A. Experimental Conditions for RTD without Baffles

flow rate Q (mL/min) [feed tube Reynolds number]	mixer rpm	mean residence time t_m (min)	σ/t_m	V (mL)	V/Q (min)	impeller Reynolds number
110 [1688]	0	18.898	0.636	1290	12.73	
	10.2	15.941	0.665	1290	12.73	395
	30	12.275	0.964	1290	12.73	1163
	49.7	11.749	0.978	1290	12.73	1927
	69.5	11.658	1.011	1290	12.73	2675
	90.6	11.607	1.021	1292	12.73	3513
	190	11.646	1.003	1294	12.73	7367
	286.7	11.757	1.026	1298	12.73	11 120
225 [3454]	0	8.086	0.746	1290	6.22	
	9.8	7.259	0.819	1290	6.22	380
	29.7	6.263	0.915	1290	6.22	1152
	50.2	5.933	0.965	1290	6.22	1946
	70	5.96	0.988	1290	6.22	2714
	91.6	5.672	1.011	1292	6.22	3551
	190.6	5.781	1.015	1294	6.22	7390
	288	6.104	1.007	1298	6.22	11 170
295 [4,528]	0	5.322	0.863	1290	4.75	
	11	4.704	0.939	1290	4.75	426
	30.2	4.242	1.017	1290	4.75	1171
	50.5	4.414	0.974	1290	4.75	1958
	69.9	4.417	1.016	1290	4.75	2710
	90	4.316	1.047	1292	4.75	3489
	188.5	4.27	1.024	1294	4.75	7308
	290	4.417	1.041	1298	4.75	11 240
400 [6,140]	0	4.147	0.866	1290	3.50	
	10.5	3.777	0.890	1290	3.50	407
	30.5	2.964	0.920	1290	3.50	1183
	51	3.211	1.009	1290	3.50	1977
	70.7	3.24	0.978	1290	3.50	2741
	89.8	3.192	1.004	1292	3.50	3482
	190	3.167	1.043	1294	3.50	7367
	287	3.383	1.060	1298	3.50	11 130
530 [8,136]	0	3.528	0.743	1290	2.64	
	9.7	3.277	0.746	1290	2.64	376
	30	2.665	0.879	1290	2.64	1163
	50	2.721	0.899	1290	2.64	1939
	70	2.53	0.883	1290	2.64	2714
	90	2.427	0.981	1292	2.64	3489
	189.5	2.393	1.043	1294	2.64	7347
	288	2.445	1.061	1298	2.64	11 170

B. Experimental Conditions for RTD with Baffles

flow rate Q (mL/min) [feed tube Reynolds number]	mixer rpm	mean residence time t_m (min)	σ/t_m	V (mL)	V/Q (min)	impeller Reynolds number	impeller power number
20 [307]	0	92.064	0.848	1400	70		
	9.7	87.915	0.867	1400	70	376	1 194 000
	29.6	77.882	0.945	1400	70	1148	48 290
	49.1	77.515	0.923	1400	70	1904	10 990
	70	72.997	0.983	1400	70	2714	3649
	88.1	73.005	1.007	1400	70	3416	1668
	188	73.632	0.989	1400	70	7289	249
	284.7	73.595	0.989	1400	70	11 040	108
40 [614]	0	44.241	0.786	1400	35		
	11.5	41.429	0.919	1400	35	446	729 500
	31.5	38.922	0.945	1400	35	1221	40 370
	50.9	36.9	0.968	1400	35	1973	9866
	69.9	37.709	0.969	1400	35	2710	3666
	91.6	35.787	0.999	1400	35	3551	1524
	190	35.396	0.992	1400	35	7367	243
	286	36.674	1.005	1400	35	11 090	107

increase from time zero and the roughness of the increases clearly indicate parasitic mixing behavior as compared to the ideal mixing curve since it should increase abruptly in an instantaneous rise at time zero and decay exponentially with time thereafter. The RTD is obtained from these experimental data by normalization in the typical manner.[6]

$$E(t) = \frac{C(t) - C(t=0)}{\int_0^\infty [C(t) - C(t=0)]dt} \tag{1}$$

where $C(t)$ represents the concentration (or temperature) trace, e.g., Figures 2 and 3. An example of the RTD is plotted in Figure 4. Even for this good mixing case there are deviations from ideal mixing at short residence times where the initial rise is not immediate and is not a smooth curve. This figure also contains a plot of the ideal RTD for the stirred tank for comparison purposes. The mean residence time (t_m) was calculated by integrating the RTD as follows[1]

$$t_m = \int_0^\infty tE(t)dt \tag{2}$$

The variance, or square, of the standard deviation of the RTD is calculated using:

$$\sigma^2 = \int_0^\infty (t - t_m)^2 E(t)dt \tag{3}$$

The magnitude of this 2nd moment is an indication of the spread of the RTD. In Figure 5 the mean

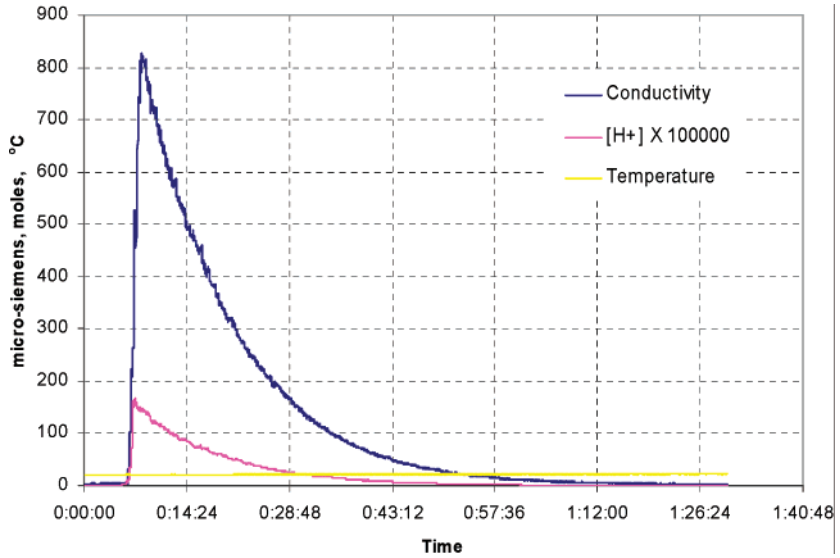

Figure 2. Concentration profile measured with conductivity, hydrogen ion concentration, and temperature for the operating conditions of flow rate 110 mL/min and mixer speed 0 rpm for a tank without baffles.

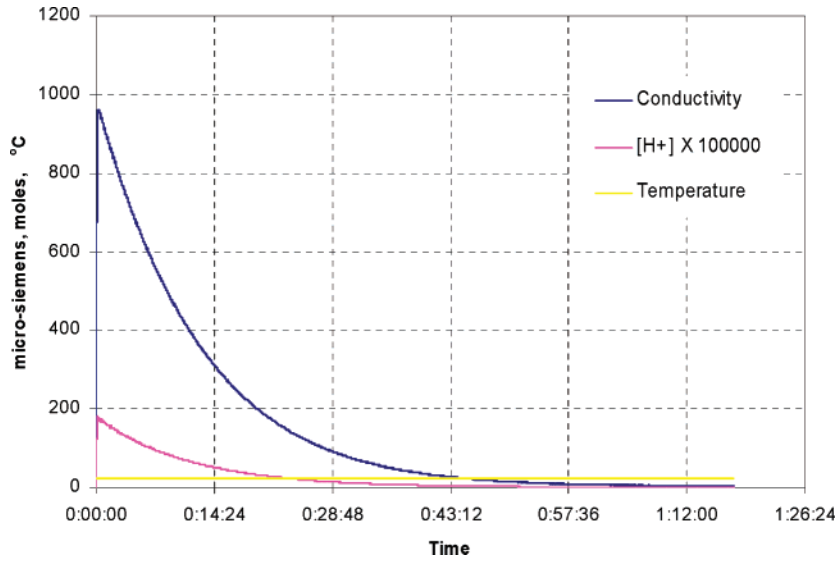

Figure 3. Concentration profile measured with conductivity, hydrogen ion concentration, and temperature for the operating conditions of flow rate 110 mL/min and mixer speed 287 rpm for a tank without baffles.

residence time obtained from the experimental data is plotted as a function of mixer rpm for various feed flow rates for the tank without baffles. Here we see that the mean residence time decreases with increasing rpm until a constant value is reached. This constant value is approximately V_{tank}/Q, the space-time for the reactor, where V_{tank} is the reactor volume and Q is the volumetric flow rate. The error in the calculation of the mean residence time, t_m, is ~8% of V_{tank}/Q for all experiments and was determined by experiments done in duplicate and some in triplicate. These errors are due to the variations in tank volume caused by the liquid level control (±3.9 mm corresponding to ±41 mL) and to the variations in the flow rate caused by a small calibration drift and pulsating peristaltic pump flow. In Figure 6, the variance of the RTD divided by the space−time is plotted as a function of mixer rpm for various feed flow rates for the tank without baffles. The error in the variance of the residence time divided by the mean residence time is ~12% at all rpm values and is larger than the mean residence time because two integrals with their inherent errors are involved in the variance divided by mean residence time calculation. For an ideal reactor the value of σ/t_m should be 1.0, which is observed, within experimental error, at higher impeller rpms. With Figures 5 and 6 one can see that mixer speed of 100 rpm was enough to approach perfect mixing for the unbaffled tank. With baffles, the results are shown in Figures 7 and 8 and the results are similar to those without baffles, however, the approach to ideal reactor behavior takes place at ~60 rpm as measured by σ/t_m, which is lower than that for the tank without baffles.

CFD Predictions. A model of the stirred tank shown in Figure 1 was constructed in Fluent's geometry and grid generation tool using a rotating mesh in the region of the impeller and a fixed mesh elsewhere. The mesh generated contains 626 512 elements. This grid was then loaded into Fluent 6.1 for resolution of the fluid flow within the tank. The standard $k-\epsilon$ turbulent model with standard wall functions was chosen to predict the flow profile; even in the case of zero rpm, since the $k-\epsilon$ model reduces to laminar flow model when the energy dissipation rate, ϵ, and the turbulent kinetic energy, k,

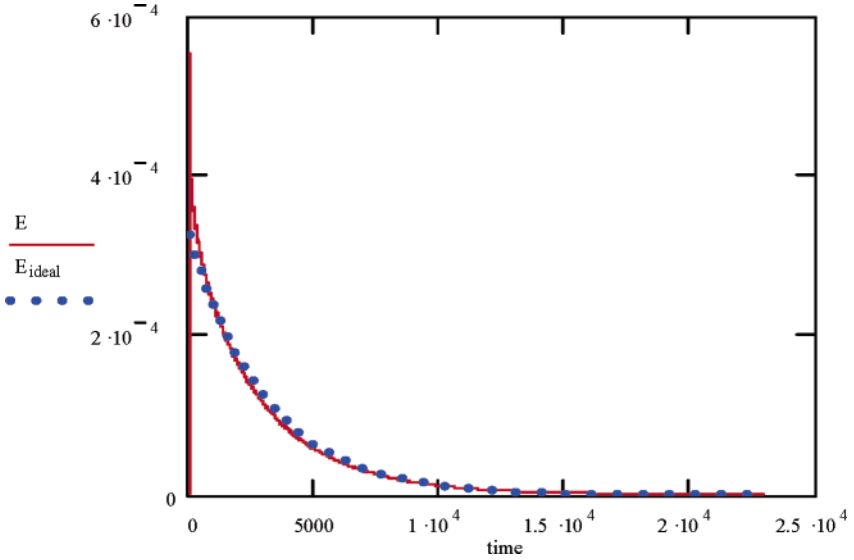

Figure 4. RTD measured with the H^+ concentration for the operating conditions of flow rate 110 mL/min and mixer speed 287 rpm for a tank without baffles.

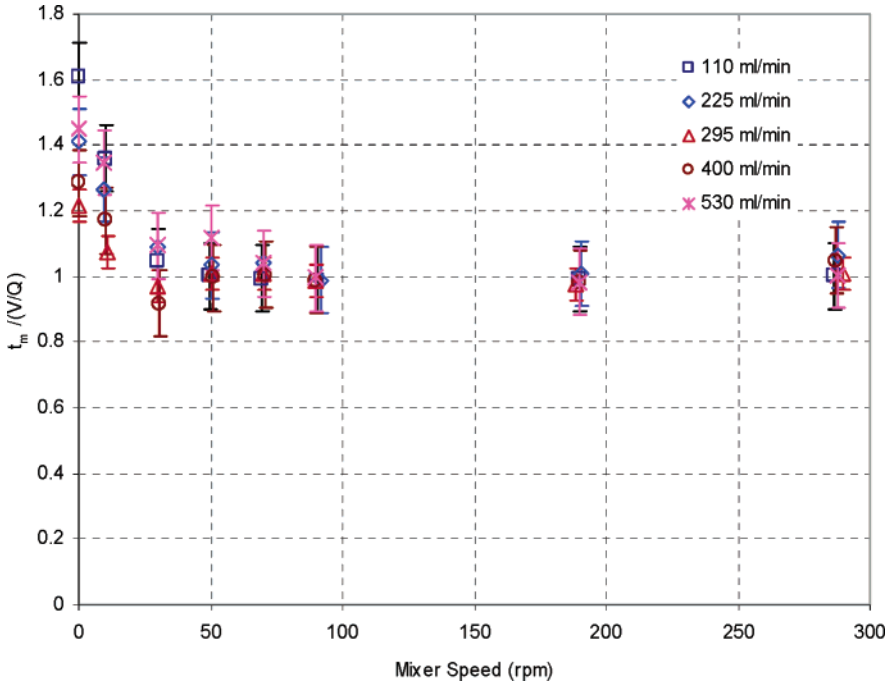

Figure 5. Mean residence time versus mixer rpm at different flow rates for ~1.3-L laboratory reactor without baffles.

are zero. The experimental conditions are for the most part in the transition flow regime (i.e., impeller Reynolds number greater than 10, considered to be laminar, and less than 10 000,[19] considered to be fully turbulent), see Table 2b, with one case in the fully turbulent regime and one in the laminar regime. The simulations were performed for laminar (0 rpm) and transition (20, 40, 80, and 200 rpm) flow regimes. The boundary condition assumed for the flow at the inlet corresponds to plug flow. The flow rate in the inlet tube is laminar in all cases for the baffled tank (see Table 2b) and has an average velocity of 0.33 m/s for a feed flow rate of 40 mL/min, and 0.17 m/s for a feed flow rate of 20 mL/min. The 0.17 m/s average feed velocity is larger than the impeller tip velocity in the 0, 20, 40, and 80 rpm simulations and the 0.33 m/s average feed velocity is larger than the impeller tip velocity in the 0, 20, and 40 rpm simulations. The tank output was given a pressure outlet boundary condition with no slip. The walls of the tank, baffles, and the other tank internals were assigned standard wall function boundary conditions, the top surface was assigned a symmetry boundary condition, the surface of the moving zone was assigned an interface boundary condition, and the surface of the impeller was assigned a (stationary) standard wall function inside the mesh that is rotating. The model was allowed to run using double precision calculations until all the scaled residuals reached a value of 10^{-4}. This level of convergence took ~1100 iterations. The resulting velocity profile is given in Figure 9 and shows that the steady-state solution contains two major circulation cells − one above and one below the impeller. The overall flow pattern in each circulation cell is that of a helical path on the surface of a torus, circulating from the impeller to the tank wall, up or down the tank wall (up for the upper circulation

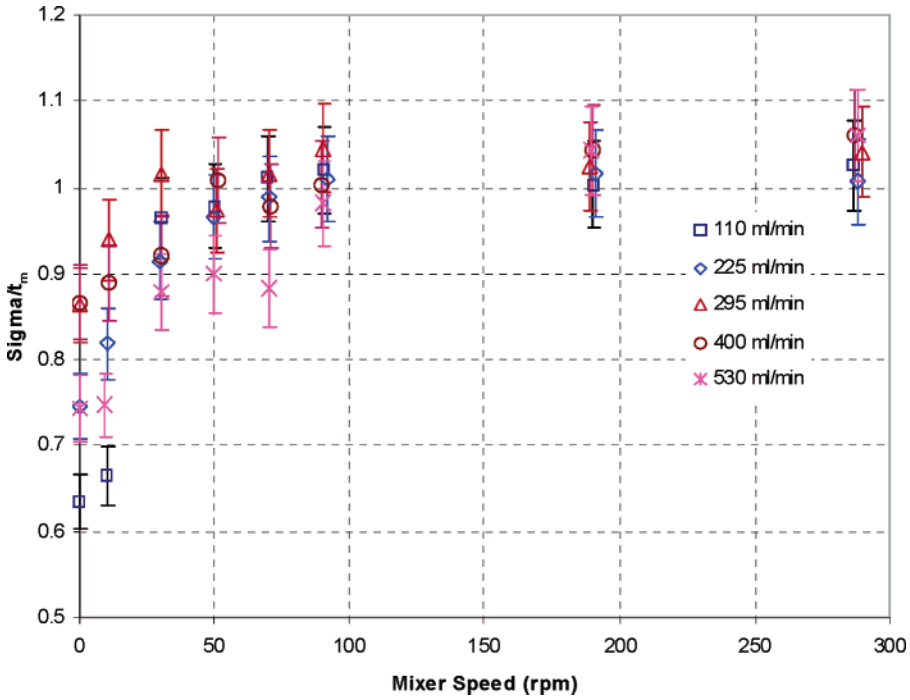

Figure 6. Comparison of σ/t_m with different flow rate and mixer rpm for a 1.3-L stirred tank without baffles.

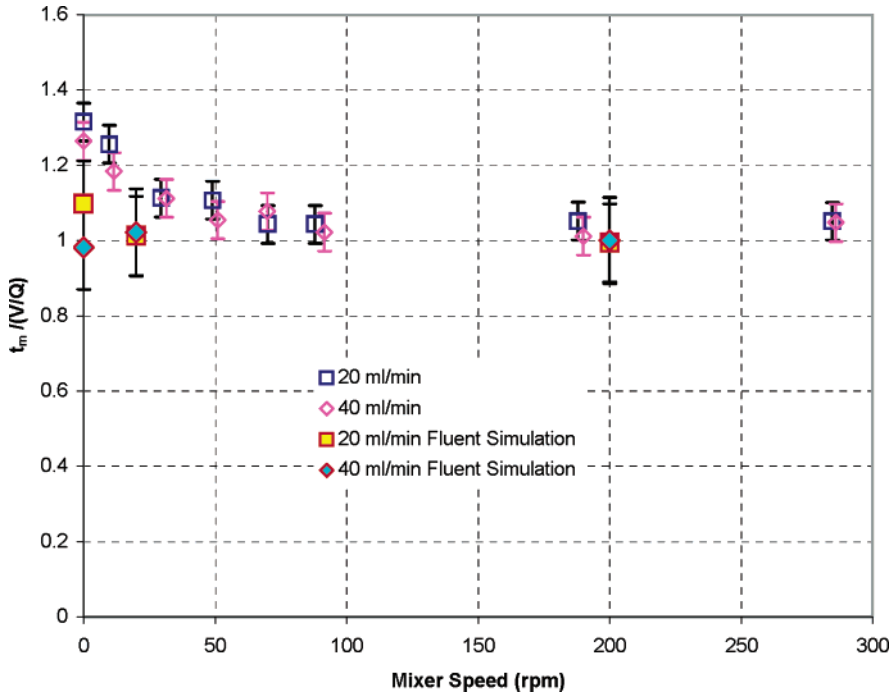

Figure 7. Mean residence time versus mixer speed at various flow rates for a 1.4-L laboratory reactor with baffles. The larger filled symbols are for the Fluent simulation results.

cell and down for the lower circulation cell), back into the center of the tank and into the impeller again. This overall flow pattern is interrupted by the flow around and behind the baffles. The flow behind the baffles plays an important role in passing fluid from the top circulation cell to the bottom circulation cell as there is a minor circulation cell of cylindrical form behind each baffle in which the material can enter from the top circulation cell and exit into the bottom circulation cell or vice versa. There is also some mixing of material between the two circulation cells at the plane of the impeller. As the flow moves radially out some of the fluid is exchanged from the upper circulation cell to the lower circulation cell and vice versa. This later mechanism operates in the tanks both with and without baffles.

The behavior of the tracer is modeled by fixing the fluid flow field and adding a user defined scalar to model the concentration of tracer with a diffusion coefficient of 10^{-5} cm^2/s. No source term was used for the user-defined scalar nor any turbulent diffusivity. The boundary conditions for the tracer consist of a feed of mass fraction of 1.0 and an output of whatever concentration is at the outlet tube located at the top of the tank. All the tank internals use a zero flux boundary condition. The initial condition for this unsteady simulation was to fill the tank with zero concentration of tracer and feed

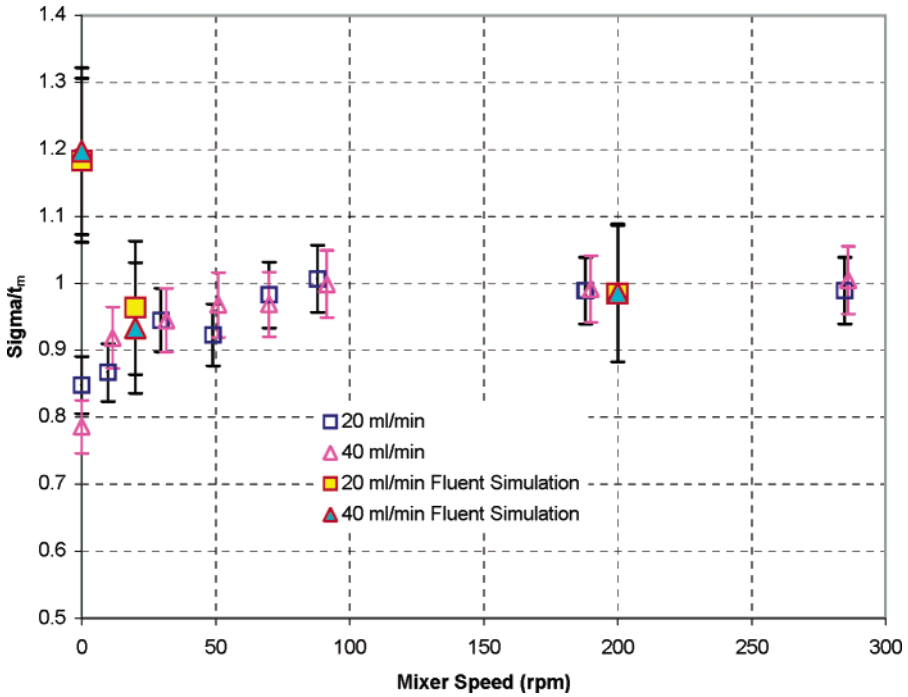

Figure 8. Standard deviation of the RTD versus mixer speed for a 1.4-L laboratory reactor with baffles. The larger filled symbols are for the Fluent simulation results.

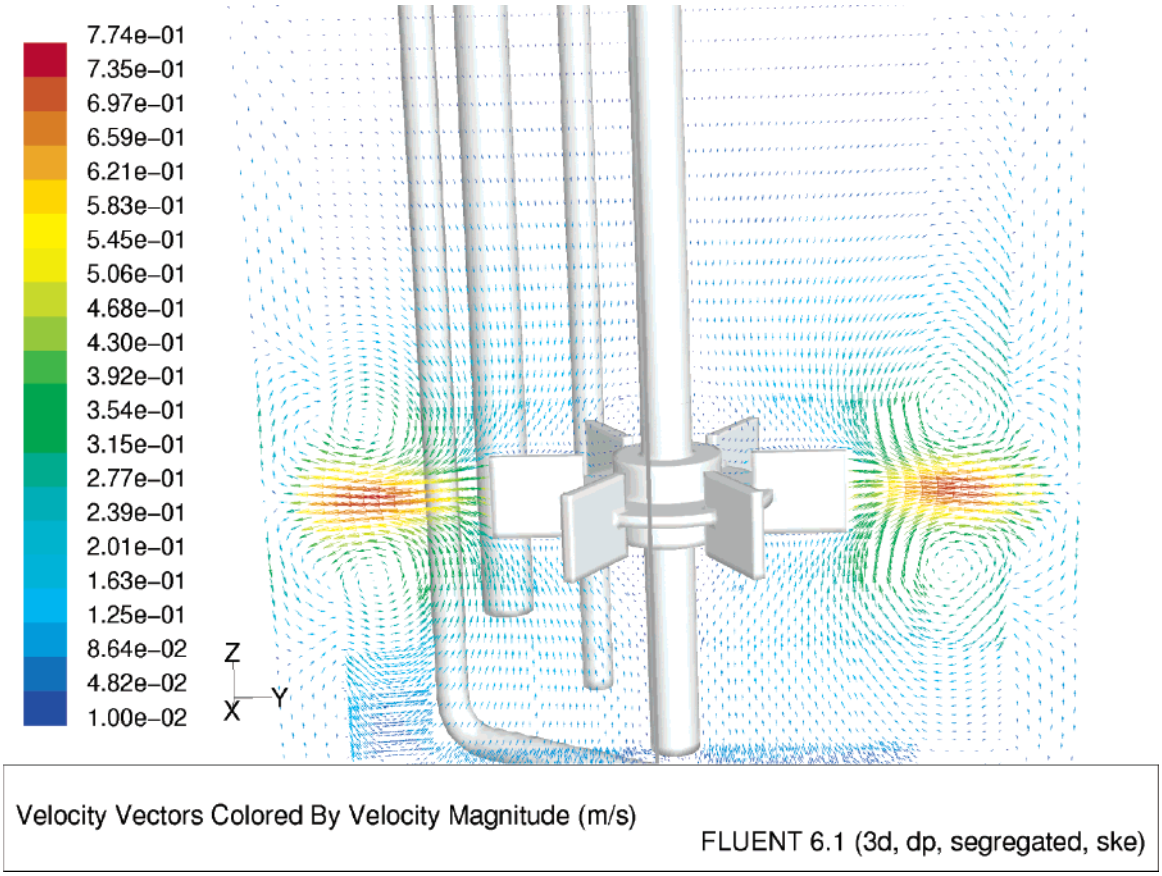

Figure 9. Velocity vector profile for turbulent flow in the 1.4-L laboratory reactor operating at 40 mL/min feed flow rate and a mixer speed of 80 rpm.

the tank with a solution with a mass fraction of 1.0 from the feed tube located just below the impeller. The simulation was allowed to precede using time steps of 20 s with the same convergence criterion. An overall mass balance was verified to be accurate to within the convergence criterion. The convective flux of the tracer at outlet is collected from this simulation and plotted against time as shown in Figure 10 where runs for several rpm values at a flow rate of 40 mL/min are plotted. Here we see that initially the concentration of tracer is zero and increases with time until the tracer concentration approaches that of the feed, a value of 1.0. This

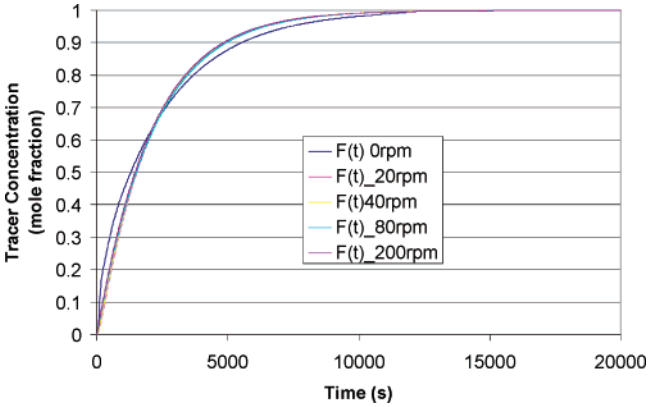

Figure 10. Output concentration as a function of time for the Fluent prediction of the residence time distribution for various mixer speeds (i.e., 0, 20, 40, 80 and 200 rpm) and a feed flow rate of 40 mL/min.

type of plot is characteristic of the response of a stirred tank reactor to a step input. The residence time distribution is obtained from this plot of tracer concentration by differentiating the curve with respect to time, i.e.

$$E(t) = \frac{dC(t)}{dt} \tag{4}$$

The RTD determined in this way is normalized since the feed tracer concentration was 1.0. This step input is a different way to determine the RTD than that used in the experiments, which was a pulse input. In attempting to use a pulse input method in the simulations, the concentrations were very small and round off errors were sufficiently large to invalidate the overall mass balance for the reactor significantly beyond the convergence criterion. Mass balance errors have been shown to cause drastic errors in RTD measurements.[20] For this reason, the step method of determining the RTD is used in these simulations.

A comparison of the Fluent-predicted RTD and that measured experimentally is shown in Figure 11 a−c for different impeller rpm values for 40 mL/min flow rate with the baffled tank. The predictions show similar trends in that there is a delay before the RTD increases after time zero and there is an initial roughness in the curve. The RTD then decreases exponentially with time. The prediction typically over predicts in the initial spike or two in the first tens of seconds, the experimental data, and the perfectly mixed theoretical curve.

The predictions for various flow rates and impeller rpm values were analyzed for the mean residence time and the variance of the RTD. These results (filled data points) are also plotted in Figures 7 and 8 for comparison with the experimental data. The error bars associated with the theoretical points were determined by running another simulation of the concentration breakthrough but with time steps of 10 s. The predictions show good agreement with the experimental data for all flow rates and rpm values except zero rpm. The error between the experimental results and predictions is well within the error bars of the two methods of determining the mean residence time, t_m, and the variance (σ) of the RTD. As a result, the Fluent predictions of the RTD for a stirred tank reactor with a complex internal geometry operating in transitional turbulent flow has been shown to give an adequate approximation of experimental measurements when the stirrer is operating. When the

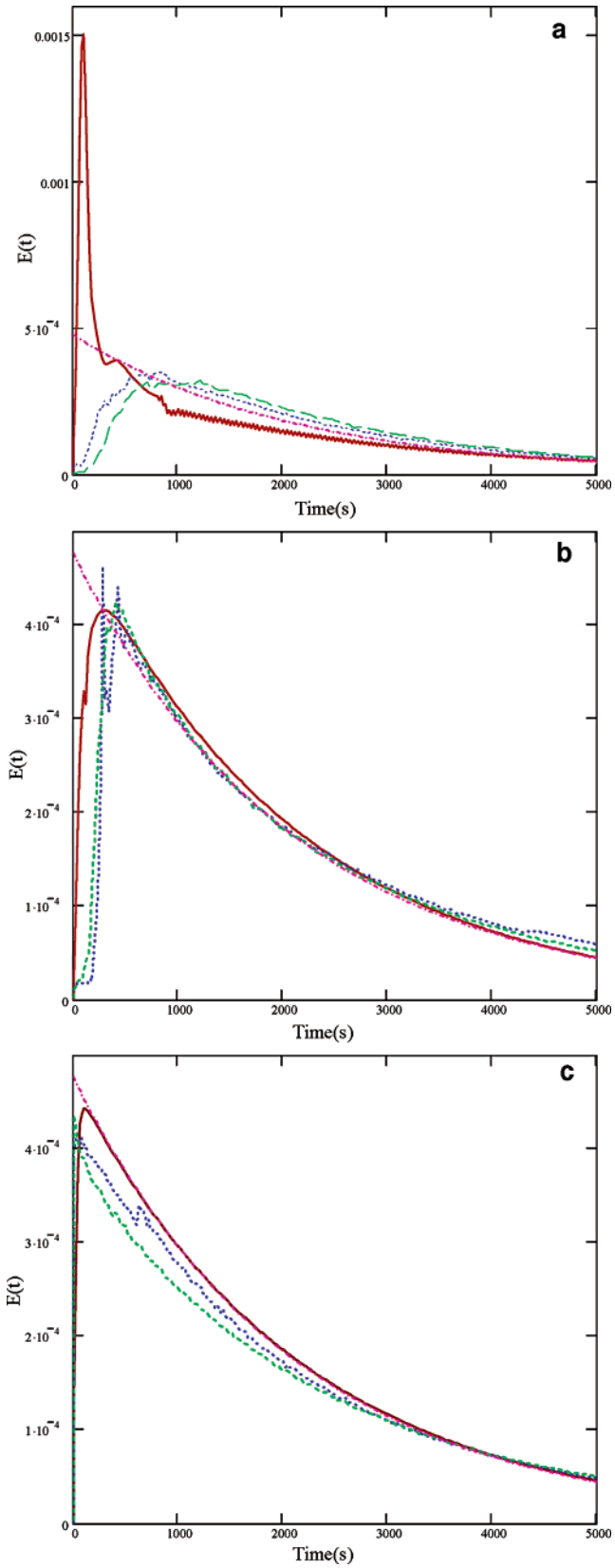

Figure 11. Comparison of experimental result of residence-time distribution function, $E(t)$, experimental measurements, and calculated ideal $E(t)$ for a perfectly mixed CSTR: (a) 0 rpm, 40 mL/min flow rate, 0 impeller Reynolds number, (b) 20 rpm, 40 mL/min, 775 impeller Reynolds number, and (c) 200 rpm, 40 mL/min, 7750 impeller Reynolds number. The red line indicates the Fluent simulation, the magenta dot−dash line indicates the perfectly mixed CSTR, the green line indicates the conductivity data, and the blue dotted line indicates the H+ concentration obtained from the pH data.

stirrer is operating the fluid flow profile is caused by the impeller as shown in Figure 9. Without the stirrer operating the fluid flow is driven by the jet of fluid entering the vessel from the feed tube, i.e., the curved tube that ends just below the impeller that provides a complicated fluid flow profile. The fluid flow profile will depend on the location of the vanes of the stopped impeller relative to the other tubes inside the tank and this location may change until the flow becomes stabilized. The location of the impeller vanes with respect to the feed tube was not noted in the experiments and could not be used for a fixed solid boundary condition in the CFD prediction. As a result the Fluent CFD prediction is inaccurate when the impeller is not rotating.

No simulations of the unbaffled tank were performed. We were focusing our work on the baffled tank since it is most commonly used in industry. Furthermore, our nonbaffled tank has 3 inlet tubes in an odd geometry that act as crude and poorly characterized baffles. In retrospect, due to more deviations in concentration from an ideal stirred tank, the simulation of the nonbaffled tank may have been a better choice to validate the CFD predictions of concentration. We did not predict the pulse concentration with time leaving the reactor in our simulations but the step concentration. So direct comparisons would not have been possible. In further consideration, the nonbaffled experiments have a larger amount of error associated with them than the baffled experiments, so that validation with respect to mean and variance of the residence time would not have been as good as that with the nonbaffled tank experiments. As a result, we think that, given these considerations, our work does an adequate job in proving the value of Fluent simulations for the prediction of residence time distributions in complicated tank geometries operating in the transitional flow regime.

Conclusions

The mean and variance of the residence time distribution for a stirred tank deviate from ideal values at low impeller rpm. As the impeller rpm is increased, the mean and variance of the residence time distribution approach the ideal values. For the nonbaffled tank ideal behavior is observed at ∼100 rpm or an impeller Reynolds number of 3878 and above, while for the baffled tank ideal behavior is observed at ∼60 rpm or an impeller Reynolds number of 2327 and above using a Rushton turbine impeller. Predictions of the RTD and its mean and variance using CFD with a $k-\epsilon$ model of turbulence show good agreement with experiment for transitional turbulent flow regimes in the tank.

Acknowledgment

We acknowledge the help of Dr. Christine Wolfe and Dr. Anupam Jain, both of Fluent, who were responsible for mesh improvements that were critical to the success of this project.

Nomenclature

$C(t)$ = concentration as a function of time
$E(t)$ = residence time distribution function
t = time
V_{tank} = volume of the reactor
Q = flow rate in to and out of the reactor

Literature Cited

(1) Fogler, H. S. *Elements of Chemical Reaction Engineering*, 3rd ed.; Prentice Hall PTR: Upper Saddle River, NJ, 1999.

(2) Khang, S. J.; Levenspiel, O. New scale-up and design method for stirrer agitated batch mixing vessels. *Chem. Eng. Sci.* **1976**, *31* (7), 569−577.

(3) Zaloudik, P. Mixed model for continuous stirred tank reactor with viscous fluid from experimental age distribution study. *React. Eng.* **1969**, *14* (5), 657−659.

(4) Gianetto, A.; Cazzulo, F. Continuous-flow mixers: working efficiency and conditions for attaining scale-up; Notes I, II and III. *Sci. Chim.* **1968**, *38* (4), 322−342.

(5) Bates, R. L. Impeller Characteristics and Power. In *Mixing: Theory and Practice*; Uhl, V. W., Gray, J. B., Eds.; Academic Press: New York, 1966; Chapter 3.

(6) Levinspiel, O. *Chemical Reactor Engineering*; Academic Press: New York, 1972.

(7) Turner, J. C. R. The interpretation of residence-time measurements in systems with and without mixing, *Chem. Eng. Sci.* **1971**, *26*, 549−557.

(8) Levenspiel, O.; Lai, B. W.; Chatlynne, C. Y. Tracer curves and the residence time distribution. *Chem. Eng. Sci.* **1970**, *25*, 1611−1613.

(9) Levenspiel, O.; Turner, J. C. R. The interpretation of residence-time experiments. *Chem. Eng. Sci.* **1970**, *25*, 1605−1609.

(10) Beltran, F. J.; Gonzalez, M.; Adedo, B.; Gomez, C. Kinetic modeling of aqueous trichloroethylene direct ozonation in a continuous tan. *J. Environ. Sci. Health Part A* **1997**, *32* (9−10), 2471−2482.

(11) Amanulla, A.; McFarlane, C. M.; Emery, A. N.; Nienow, A. W. Scale-down model to simulate spatial pH variations in large-scale bioreactors. *Biotechnol. Bioeng.* **2001**, *73* (5), 390−399.

(12) Li, K. T.; Lee, J. D. Mixing and control of a CSTR with series-parallel reactions. *J. Chin. Inst. Chem. Eng.* **1991**, *22* (2), 61−69.

(13) Newell, B.; Bailey, J.; Islam, A.; Hopkins, L.; Lant, P. Characterizing bioreactor mixing with residence time distribution tests. *Water Sci. Technol.* **1998**, *37* (12), 43−47.

(14) Randolph, A. D.; Bechman, J. R.; Kraljevich, K. Crystal size distribution dynamics in a classified crystallizer: Part I. Experimental and theoretical study of cycling in a potassium chloride crystallizer. *AIChE J.* **1977**, *23* (4), 500−510.

(15) Walas, S. M. Rules of thumb. *Chem. Eng.* **1987**, March 16, 75−81.

(16) Myers, K. J.; Reeder, M. F.; Fasano, J. B. Optimize mixing by using the proper baffles. *Chem. Eng. Prog.* **2002**, *98* (2), 42−47.

(17) Johnson, J. L.; Fan, L. T. Observation concerning Pulse testing of flow systems. *AIChE J.* **1966**, *12*, 1026.

(18) Video clips of these experiments are available at http://www.che.utah.edu/∼ring/CrystallizationWeb/RTD Videos/dads ex 3.mov.

(19) Perry, R. H.; Chilton, C. H. *Chemical Engineers' Handbook*, 5th ed.; McGraw-Hill: New York, 1973.

(20) Curl, R. L.; McMillan, M. L. Accuracy in Residence Time Measurements, *AIChE J.* **1966**, *12* (4), 819−822.

Received for review November 10, 2003
Revised manuscript received July 1, 2004
Accepted July 1, 2004

IE0308240